Quaternary Science Reviews 340 (2024) 108861

Contents lists available at ScienceDirect

Quaternary Science Reviews

journal homepage: www.elsevier.com/locate/quascirev

Methodological constrains of tree-ring stable isotope chronologies

Tito Arosio[a,*], Max Torbenson[b,c], Tatiana Bebchuk[a], Alexander Kirdyanov[a,d], Jan Esper[b,c], Takeshi Nakatsuka[e], Masaki Sano[f], Otmar Urban[c], Kurt Nicolussi[g], Markus Leuenberger[h,i], Ulf Büntgen[a,c,j]

[a] *Department of Geography, University of Cambridge, Cambridge, CB2 3EN, UK*
[b] *Department of Geography, Johannes Gutenberg University, 55099, Mainz, Germany*
[c] *Global Change Research Institute of the Czech Academy of Sciences, 603 00, Brno, Czech Republic*
[d] *Sukachev Institute of Forest SB RAS, 660036, Krasnoyarsk, Russian Federation*
[e] *Research Institute for Humanity and Nature, Kyoto, 603-8047, Japan*
[f] *National Museum of Japanese History, Sakura, 285-8502, Japan*
[g] *Institute of Geography, University of Innsbruck, 6020, Innsbruck, Austria*
[h] *Climate and Environmental Physics, Physics Institute, University of Bern, 3012, Bern, Switzerland*
[i] *Oeschger Centre for Climate Change Research, University of Bern, 3012, Bern, Switzerland*
[j] *Department of Geography, Faculty of Science, Masaryk University, 613 00, Brno, Czech Republic*

ARTICLE INFO

Handling editor: A. Voelker

Keywords:
Climate reconstructions
Proxy data
Stable isotopes
Spectral properties
Tree rings

ABSTRACT

Tree-ring stable isotope (TRSI) chronologies that combine information from living and relict wood have the potential to capture long-term trends that might be missing in traditional tree-ring width and maximum latewood density measurements. Our understanding of the possible effects of different methods to develop TRSI chronologies is, however, still incomplete. Here, we compare and evaluate five such methods applied to three multi-millennial-long oxygen isotope ($\delta^{18}O$) TRSI datasets from central Europe, the European Alps and Japan: (a) raw data, (b) cohort correction, (c) interactive mean correction, (d) outlier correction, and (e) series normalization. We show that the spectral properties preserved in the final TRSI chronologies not only depend on the data used, but also on the techniques applied. Method (a) is particularly prone to outliers if the sample size is low. Method (b) may create artificial steps and trends when single measurement series share similar start dates and/or when end and start dates are systematically skewed. Methods (c) and (d) yield similar results for annually resolved data, yet (d) is more suitable for temporally pooled datasets and less sensitive to potential biological age effects. Method (e) removes any low-frequency signal. Our findings demonstrate the risks and rewards of different TRSI chronology development techniques that must be carefully adapted to both, the data used and the question posed.

1. Introduction

Tree rings are valuable proxies of environmental conditions (Fritts, 1976). The limiting climatic factor of a tree's growth is recorded in the amount of wood produced in a given year, measured as tree-ring width (TRW). However, this proxy has limitations in capturing long-term climatic variations that extend beyond the lifespan of individual trees (Briffa et al., 1996; Cook et al., 1995; Esper et al., 2002, 2012, 2015). This limitation can possibly be overcome by analyzing tree-ring stable isotopes (TRSI) (Büntgen, 2022). During photosynthesis, trees incorporate into their wood the isotopic elements of carbon, oxygen and hydrogen from water and CO_2, the relative abundances of which are influenced by environmental and climate factors (McCarroll and Loader, 2004). In particular, the abundance of oxygen isotope in tree rings ($\delta^{18}O$) is mainly dependent on the water source and on the evapotranspiration in the soil and in the leaves (Treydte et al., 2014). Thus, oxygen TRSI reflects the environmental condition rather than the plant metabolic processes, and from its analysis, it is possible to obtain insights into the climatic conditions that prevailed over long timescales, potentially spanning several centuries or even millennia (Büntgen, 2022). In fact, TRSI has been used to reconstruct hydroclimate conditions in Asia and Europe over several millennia (Büntgen et al., 2021;

* Corresponding author.
E-mail address: ta530@cam.ac.uk (T. Arosio).

https://doi.org/10.1016/j.quascirev.2024.108861
Received 10 May 2024; Received in revised form 24 July 2024; Accepted 24 July 2024
Available online 31 July 2024

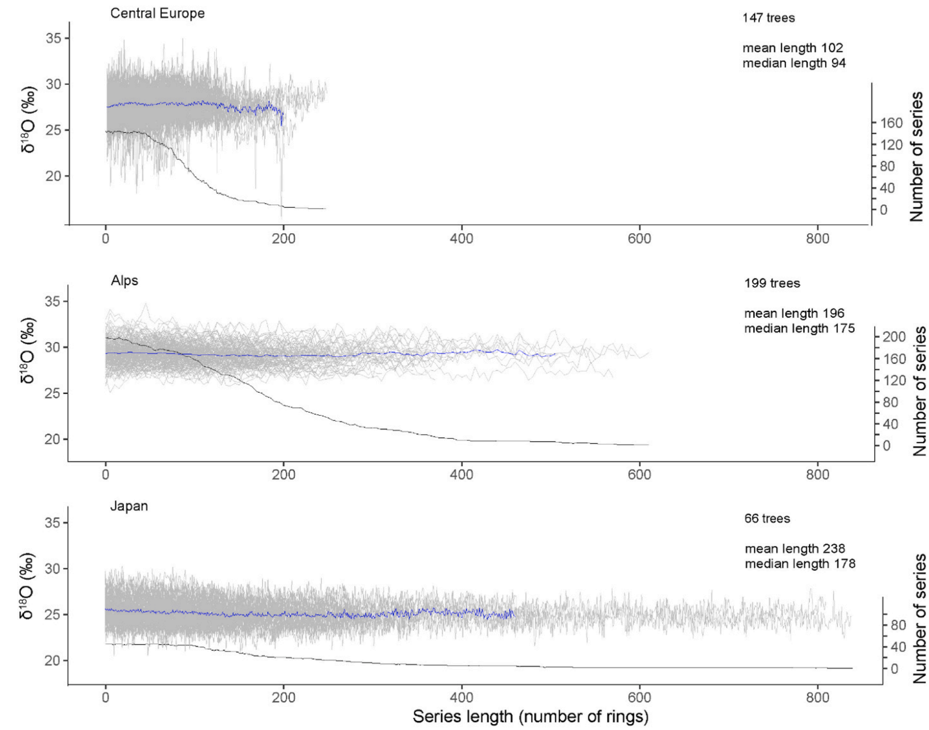

Fig. 1. Age-related plots of tree ring cellulose $\delta^{18}O$ records from Central Europe, the Alps and Japan. Gray lines represent individual tree ring $\delta^{18}O$ series, while the blue lines show the mean series for each region. The bottom axis for each region displays the number of tree ring series. The $\delta^{18}O$ ‰ values are relative to the SMOW standard. The Central European record has a mean length of 102 years (median 94 years), the Alpine record has a mean length of 196 years (median 175 years), and the Japan record has a mean length of 338 years (median 171 years).

Helama et al., 2018; Nakatsuka et al., 2020; Treydte et al., 2006; Yang et al., 2021).

TRSI chronologies do not require complete detrending since TRSI age-related trends do not span the entire cambial lifespan and are present only in the juvenile phase (Arosio et al., 2020; Büntgen et al., 2020; Duffy et al., 2019; Esper et al., 2010; Torbenson et al., 2022; Wieland et al., 2024). Moreover, they do not require procedures to stabilize variance with cambial age, as they are homoscedastic (McCarroll and Loader, 2004; Warren et al., 2001). This is an important advantage over TRW chronologies that must undergo detrending procedures to remove age-related trends and stabilize variance over time (Esper et al., 2003). However, trees may exhibit varying TRSI mean values due to microclimatic conditions or physiological factors (Leavitt, 2010), and different methods have been used to join individual tree TRSI measurements. The TRSI averaging method and the tree variability should be taken into account since potential noise can be introduced into the final chronology, considering that TRSI datasets often have a sample replication of 4–6 trees only (McCarroll and Loader, 2004). The effects of these methods on the final chronologies have not yet been systematically investigated, while much comparative work has been done on the TRW chronologies (Cook and Kairiukstis, 1990; Fritts, 1976).

The standard statistical metrics used in tree-ring research, such as inter-series correlation (R-bar) and Expressed Population Signal (EPS), focus on the relative coherence in the year-to-year signal across the tree-ring samples. These measures do not indicate the confidence intervals around the absolute mean value of the tree-ring measurements (McCarroll and Loader, 2004). Five different methods have been reported in the literature for building TRSI chronologies, and four of them include the correction of offsets between trees (Hangartner et al., 2012; Labuhn et al., 2016). Briefly, they are: (a) the use of the raw data (RAW-D); (b) the adjustment of the older cohort's mean to match the overlap mean (CO–CO); (c) the correction of offset of the individual time series compared to the mean chronology (IN–CO); (d) the correction of outlier series (OU–CO); and (e) the normalization of all trees to have the same mean of 0 (NORM). All these methods have been utilized for developing long-term paleoclimate reconstructions from TRSI. However, it remains unclear which of them produces the most robust records.

Here, we aim to better understand the process of the development of TRSI chronologies, and therefore apply the five above mentioned methods to three multi-millennial $\delta^{18}O$ TRSI datasets. Comparison of the resulting chronologies provides insights into the relationships between the features of the original datasets and the methods applied toward them.

2. Data and methods

2.1. Data and isotope measurement description

The TRSI dataset from Central Europe contains 147 oak (*Quercus* spp.) samples spanning the past 2110 years from modern-day Czech Republic and southeastern Germany (Büntgen et al., 2021). Latewood alpha-cellulose from each tree ring underwent modified Jayme-Wise isolation (Urban et al., 2021), and $\delta^{18}O$ measurements were performed at the Global Change Research Institute in Brno using an Isoprime 100 isotope ratio mass spectrometer operating in continuous flow mode with 0.1‰ analytical precision. The TRSI dataset from the European Alps contains 199 trees located at the treeline in the Swiss, Austrian, and Italian Alps between 46.03 and 47.03° N and 7.55–15.25° W (Arosio et al., 2020). The dataset contains a mix of *Pinus cembra* and *Larix decidua* samples. The dataset spans 6980 BCE (8880 BP) to 2015 CE with a five-year temporal resolution. All samples from the Alps underwent cellulose extraction (Ziehmer et al., 2018) and were analyzed for $\delta^{18}O$ isotopes at the University of Bern with 0.3‰ analytical precision. In this study, we use data for the past 6000 years only as the earlier data exhibit unusual variability, which requires special corrections (Arosio et al., 2024). The TRSI dataset from Japan contains 66 trees covering 2600 years (Nakatsuka et al., 2020). Most samples are Japanese cypress (*Chamaecyparis obtusa*) alongside other conifers like *Chamaecyparis*

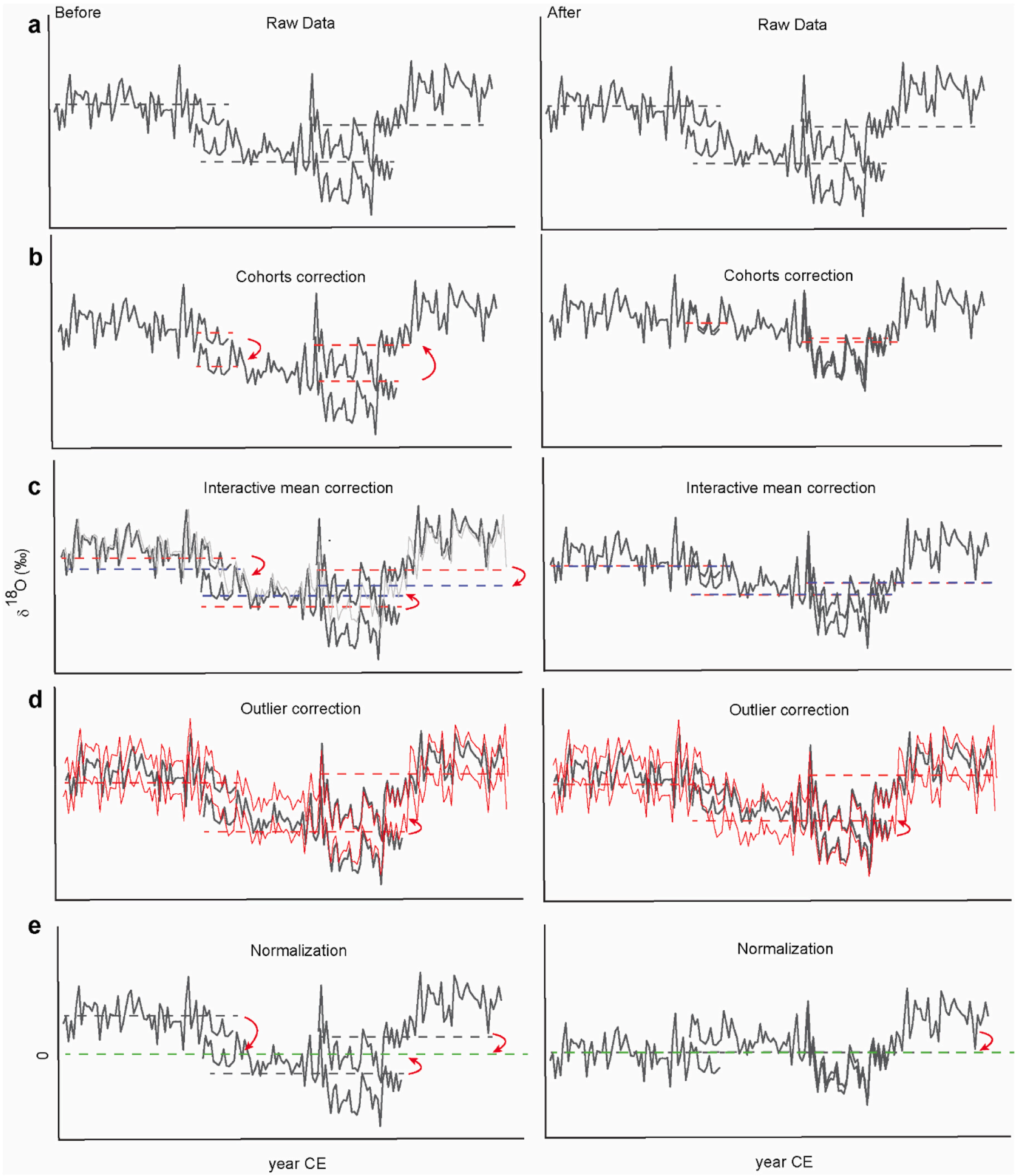

Fig. 2. Schematic $\delta^{18}O$ pseudo-proxies of three cohorts to illustrate the five correction methods. Each panel shows pseudo-proxies tree-ring $\delta^{18}O$ series (gray lines) before (left column) and after (right column) applying the specified correction method. Colored arrows highlight examples of corrections made to individual series. Horizontal dotted lines represent the mean of each individual series, while solid horizontal lines show the mean of the composite chronology at corresponding time points across aligned series.

pisifera, *Sciadopitys verticillata*, and *Cryptomeria japonica*. Cellulose was extracted with the Kagawa method (Kagawa et al., 2015) and isotopes were measured on a TCEA/Delta V Advantage mass spectrometer with 0.15‰ analytical precision. The characteristics of the three datasets are summarized in Fig. 1 $\delta^{18}O$ is a measure of the deviation in the ratio of stable isotopes oxygen-18 (18O) and oxygen-16 (16O), and is defined as the deviation in "per mil" (‰, parts per thousand) between a sample and a standard. The $\delta^{18}O$ results are reported in per mil (‰) relative to Vienna Standard Mean Ocean Water (VSMOW) for oxygen (Coplen, 1994).

2.2. *Age-related trends in raw measurements*

To investigate potential age-related trends, we aligned all individual TRSI series by their innermost ring measured. This cambial age alignment does not account for any pith offset that could affect the absolute ages assigned to each ring. We calculated mean $\delta^{18}O$ values for ring number only if the sample replication was higher than six. The resulting mean time series represents the population-level $\delta^{18}O$ variability as a function of tree age. This approach enables the examination of juvenile effects and other biological trends in the stable isotope ratios without making assumptions about year-to-year correspondence among the

Table 1
Description of the five Correction techniques methods.

Method	Names	Abbreviation	Description	References and uses
a	Raw data	RAW-D	No corrections	(Büntgen et al., 2021; Kirdyanov et al., 2008; Pumijumnong et al., 2020; Yang et al., 2021)
b	Cohort correction	CO–CO	The old tree is corrected to the young trees in the overlapping period	(Gagen et al., 2012; Hangartner et al., 2012; Naulier et al., 2015)
c	Interactive mean correction	IN-CO	The mean of the tree is corrected to the chronology mean	(Nagavciuc et al., 2022; Nakatsuka et al., 2020)
d	Outliers correction	OU-CO	Only the outlier trees are corrected	(Arosio et al., 2024; McCarroll and Loader, 2004)
e	Normalization	NORM	All the trees are corrected to have the mean of 0	(Arosio et al., 2022; Esper et al., 2018; Labuhn et al., 2016; Sano et al., 2023; Sidorova et al., 2019; Wang et al., 2020; Xu et al., 2019; Zhao et al., 2023)

individual series. None of the datasets exhibited evident long-term trends associated with cambial age (Fig. 1).

2.3. Methods for generating multi-centennial chronologies

Raw Data (method a, **RAW-D**): The uncorrected raw data from individual series are averaged to create the chronology. This method is frequently used in multi-millennial chronologies, such as the 6700-year record from the Tibetan Plateau (Yang et al., 2021) and millennial chronologies in Central Europe (Büntgen et al., 2021). No adjustments or standardization procedures are applied, preserving the original measurements.

Cohort Correction (method b, **CO–CO***)*: Proposed by Hangartner et al. (2012), and employed by Naulier et al. (2015) for a millennium-long chronology with a specific sampling strategy. This method CO–CO corrects offsets between different cohorts of tree-ring data. Adjustments are made to the mean values in the overlapping periods, aligning the older cohort's mean with that of the more recent one, while maintaining the original variance. The objective is to harmonize data across different trees or time periods, thereby creating a standardized chronology devoid of biases from overlapping data.

Interactive Mean Correction (method c, **IN-CO***)*: Proposed and applied by Nakatsuka et al. (2020) and employed by Nagavciuc et al. (2022). This iterative method is based on the recalculation of mean tree-ring values, addressing discrepancies between individual tree means and a rolling mean of the entire dataset. The process is repeated until successive iterations yield negligible changes, indicating that the chronology has stabilized and is no longer subject to internal variability.

Outlier Correction (method d, **OU-CO***)*: Proposed and applied by Arosio et al. (2024). This method targets outliers, which are time series that significantly diverge from most observations. Outlier trees are detected by calculating the chronology mean value plus or minus the variance from the calibration period. Trees with a mean value outside of this range are marked as outliers and are adjusted with an iteractive process. More specifically, half of the difference between the chronology and outlier tree mean values was subtracted, and this process was repeated until all outliers were removed.

Normalization (method e, **NORM***)*: this method is commonly used for shorter chronologies (Table 1). Each series is corrected such that its mean value is zero, without altering the variance within the series. This normalization ensures that all data series contribute equally to the final chronology, thereby facilitating the comparison between series and enhancing the overall reliability of the composite chronology.

2.4. Comparative analysis of chronologies

To assess the differences between the chronologies, a correlation analysis (Table 2), a low-frequency analysis (Fig. 6), a spectral analysis (Fig. 7), and a distribution probability analysis were conducted (Fig. 8). The Pearson correlation analysis was carried out between RAW-D and normalized NORM chronologies versus the three other correction methods: CO–CO, IN-CO, and OU-CO, for the three regions considering the time period 0 to 2000 CE.

The low-frequency analysis involved filtering the chronologies with a 300-year spline. This allowed the centennial to millennial-scale variations in the chronologies to be highlighted. The results were then compared by site (Fig. 6a, b, c) and by method (Fig. 6d,e,f,g,h).

Spectral power analysis, conducted through the fast Fourier transform method, is also a way to explore the frequency and power distributions of time series (Bloomfield and Nychka, 1992). The spectral power was calculated for each chronology, considering the time period 0 to 2000 CE. The results were then grouped by site (Fig. 6a, b, c) and by method (Fig. 6d,e,f,g,h).

The values and probability density were calculated for each chronology. Boxplots representing the distribution of values for different chronologies at different sites (Fig. 8a). The boxplot compactly displays the distribution of a continuous variable showing the median, two hinges and two whiskers (McGill et al., 1978). The kernel probability density was calculated for each chronology and was grouped and presented separately for each site (Fig. 8b). The statistical analysis was done on R studio software.

3. Results

None of the datasets exhibited evident long-term trends associated with cambial age (Fig. 1).The **Central European** and the **Alpine** datasets exhibit uniformly time series segmented lengths, showing higher sample replication in recent times (1800–2000 CE) (Figs. 3f and 4f), while the Japanese dataset displays irregular segmentation with longer samples post-1300 CE (Fig. 5f).

In the **Central European** dataset (Fig. 3), methods IN-CO and OU-CO mirrored the original RAW-D results closely, while CO–CO produced a distinct chronology, and NORM preserved only high-frequency signals. A similar pattern was observed when correcting the **Alpine** dataset: OU-

Table 2
Correlation analysis (Pearson correlation coefficient, r) between the methods. *** indicates p-values <0.001.

	Central Europe				Alps				Japan			
		CO–CO	IN-CO	OU-CO		CO–CO	IN-CO	IN-CO		CO–CO	IN-CO	OU-CO
RAW-D	0.80***	0.78***	0.98***	0.99***	0.69***	0.68***	0.45***	0.98***	0.78***	0.82***	0.96***	0.97***
NORM		0.56***	0.85***	0.85***		0.47***	0.69***	0.55***		0.51***	0.86***	0.84***

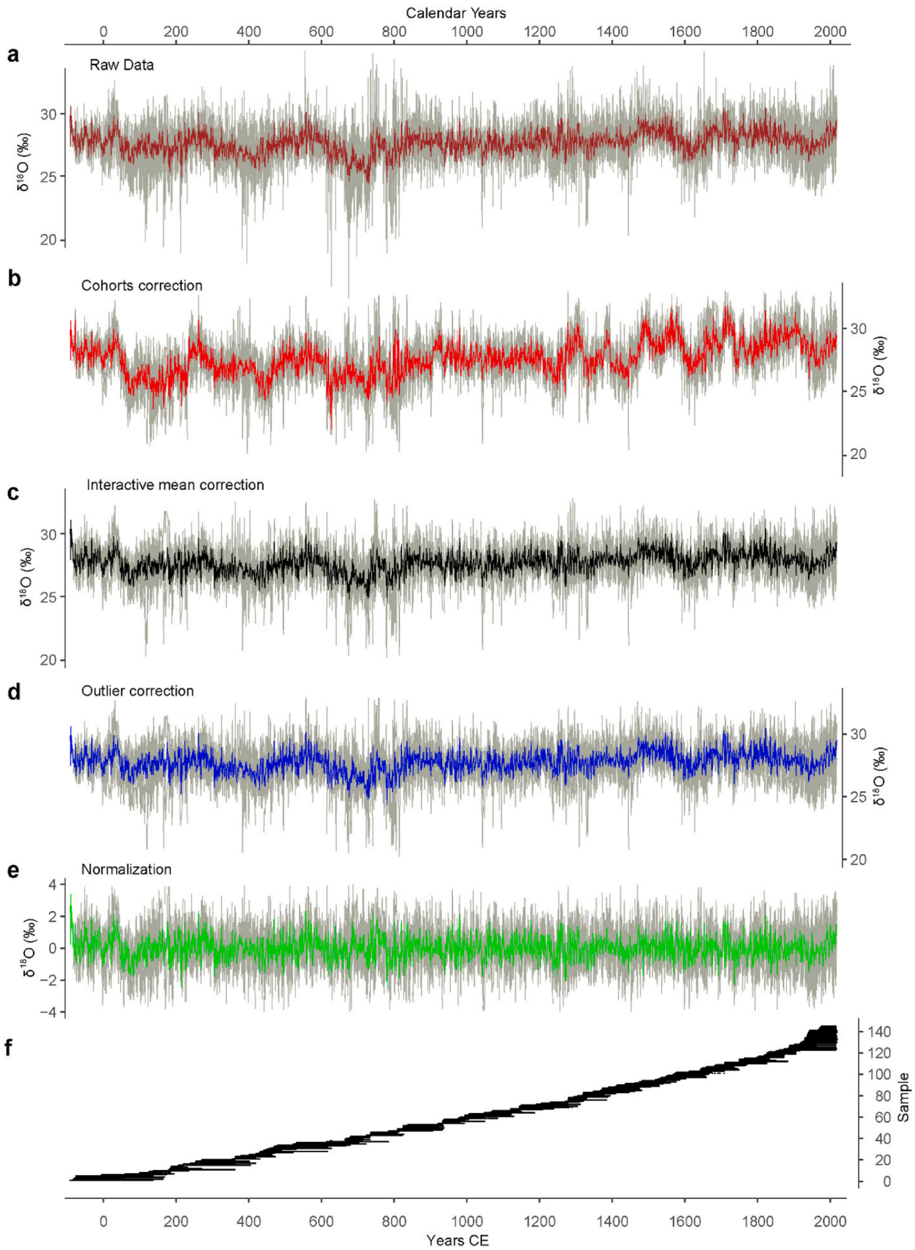

Fig. 3. Central European Chronology Corrections. Panels a to e present the dataset after a correction has been applied, with individual time series represented in gray and the aggregate average in the following colors: raw data (brown), cohort correction (red), interactive mean correction (black), correction of outliers (blue), and normalization (green). Panel f shows the temporal distribution of individual time series.

CO maintained the RAW-D chronology's integrity, IN-CO and CO–CO resulted in significantly different chronology, and NORM preserved high-frequency variability only. For the **Japanese** dataset (Fig. 5), neither IN-CO nor OU-CO significantly modified the RAW-D outcome, while CO–CO created a distinct shape in the chronology up to approximately 1300 CE. These observations highlight varied impacts, which each correction method has on dendrochronological data, with IN-CO and OU-CO showing minimal deviation from RAW-D, and CO–CO introducing distinct alterations.

Correlation anlysis (Table 2) show that for the **Central European** dataset, the RAW-D chronology closely aligned with OU-CO (r = 0.99) and IN-CO (r = 0.98), but less so with CO–CO (r = 0.79). NORM showed a high correlation with IN-CO (r = 0.86), slightly less with OU-CO (r = 0.85), and notably lower with CO–CO (r = 0.57), the correlation between RAW-D with NORM is 0.80. In the **Alpine** dataset, RAW-D had the highest correlation with OU-CO (r = 0.98), significantly lower with CO–CO (r = 0.68) and IN-CO (r = 0.45). NORM's correlation with RAW-D was modest (r = 0.52), highest with IN-CO (r = 0.69), followed by OU-CO (r = 0.55), and lowest with CO–CO (r = 0.45); the correlation between RAW-D with NORM is 0.69.

The **Japanese** dataset showed RAW-D most closely correlated with IN-CO (r = 0.98) and OU-CO (r = 0.97), and less with CO–CO (r = 0.82). NORM exhibited a high correlation with IN-CO (r = 0.86) and OU-CO (r = 0.84) and lowest with CO–CO (r = 0.51), indicating varied degrees of similarity and divergence among the methods across datasets. The correlation between RAW-D and NORM is 0.78.

3.1. *Low-frequency analysis*

To analyze the low-frequency, a 300-year spline was applied to the chronologies. This approach highlighted the impact of correction methods on generating long-term trends and variability over centuries

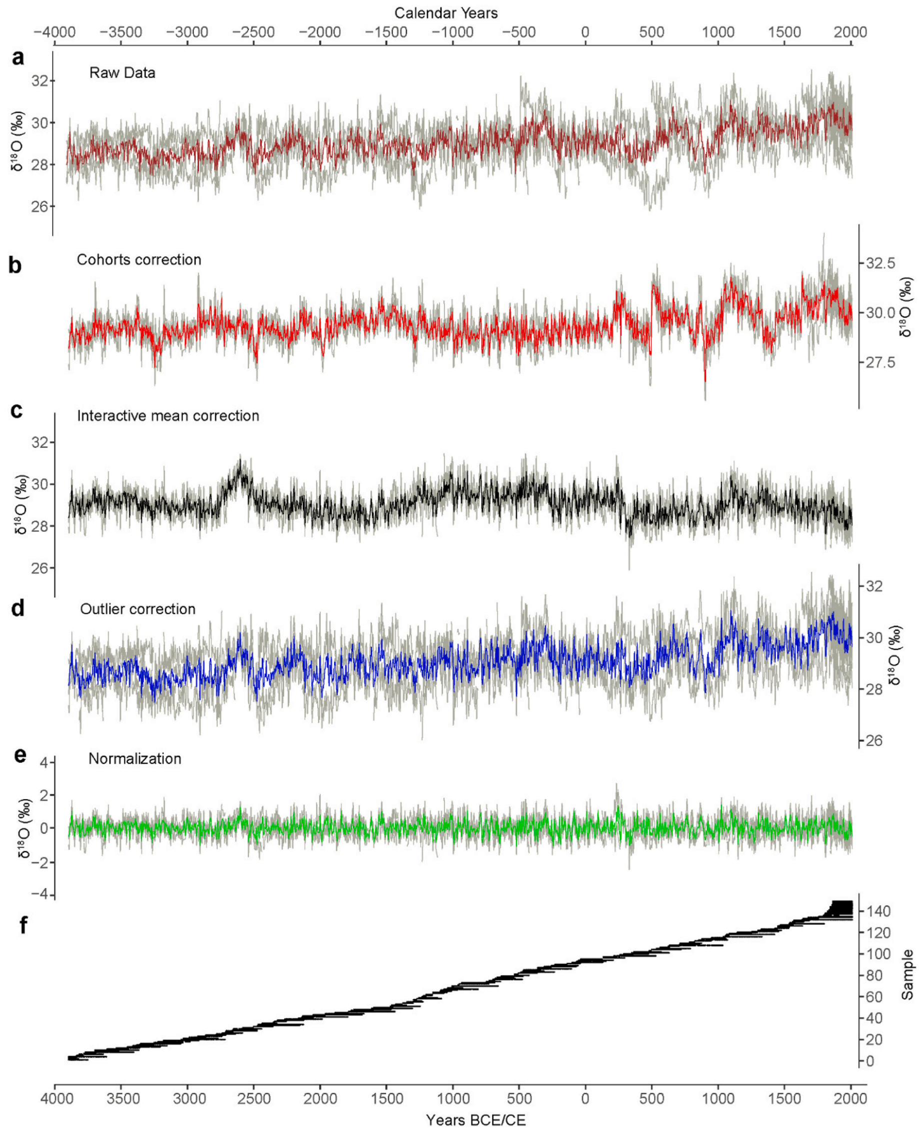

Fig. 4. Alpine Chronology Corrections. Panels a to e present the dataset after a correction has been applied, with individual time series represented in gray and the aggregate average in the following colors: raw data (brown), cohort correction (red), interactive mean correction (black), correction of outliers (blue), and normalization (green). Panel f shows the temporal distribution of individual time series.

to millennia. In the **Central European** dataset (Fig. 7a), the RAW-D, IN-CO, and OU-CO methods produced similar low-frequency signals, suggesting a consistency in capturing long-term trends. However, the NORM method significantly removed these low-frequency signals, while the CO–CO method revealed more pronounced trends than the other methods. For the **Alpine** dataset (Fig. 7b), RAW-D and OU-CO methods showed congruence in low-frequency signal representation. The IN-CO method's results diverged, and like as in Central Europe, NORM largely eliminated low-frequency signals. The IN-CO method applied to the **Alpine** dataset displayed distinct downward and upward trends, which become stronger as the iteration is repeated more times (S1). The **Japanese** dataset exhibited similar patterns to Centraler Europe in terms of the near-complete removal of low-frequency signals by the NORM method and a unique signal profile produced by the CO–CO method (Fig. 7c).

Overall, the NORM method consistently removed low-frequency signals (Fig. 7h), whereas the CO–CO method consistently introduced or highlighted distinct long-term trends.

3.2. Spectral analysis and autocorrelation analysis

To understand how the spectral profiles of the chronologies are affected by the correction methods, we conducted a spectral analysis comparing different methods (Fig. 7a, b and c), and regions (Fig. 7d, e, f and g). At all three sites, all the chronologies increased the spectral power with increasing periods. In all chronologies in the **Alpine** and **Centeal European** datasets (Fig. 7a, b), the power increased with the period in, except for the NORM method, which reduced the spectral power over periods longer than the average segment length. In the **Japanese** dataset (Fig. 7c)., the power of the signal did not increase with the period. In the cross-region comparison (Fig. 7d, e, f and g), the **Alpine dataset** showed a reduced power at the low frequencies in all chronologies.

The autocorrelation analysis (Table 3) indicates that across all three datasets, method CO–CO has the highest autocorrelation, while normalization has the lowest. Methods IN-CO and OU-CO have similar autocorrelation values compared to the RAW-D data chronology.

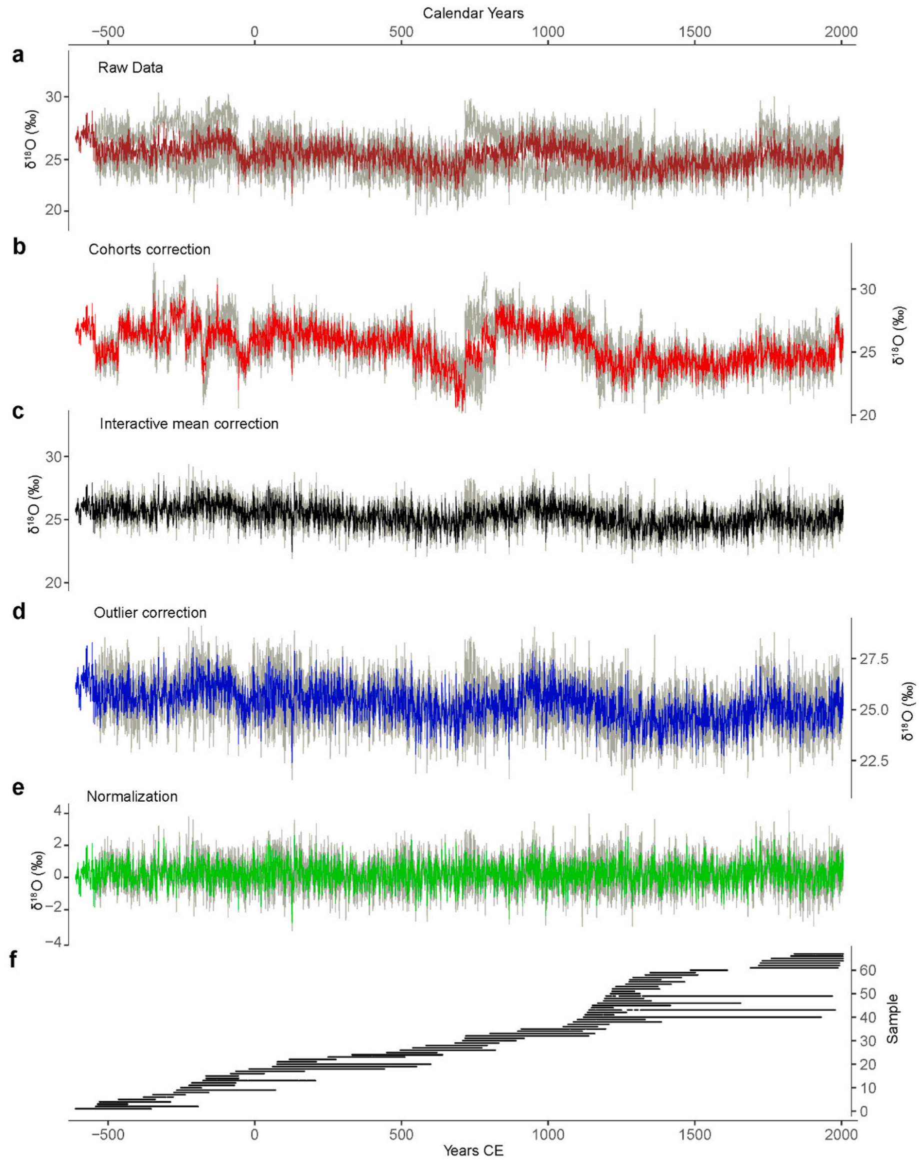

Fig. 5. Japan Chronology Corrections. Panels a to e pesent the dataset after a correction has been applied, with individual time series represented in gray and the aggregate average in the following colors: raw data (brown), cohort correction (red), interactive mean correction (black), correction of outliers (blue), and normalization (green) Panel f shows the temporal distribution of individual time series.

3.3. Mean value and density distribution

The box plot (Fig. 8a) shows that the values of the final chronologies obtained by the five correction methods and from the three sites are generally within a similar range, except for the NORM method. For the NORM method, the mean value is 0, while the CO–CO and IN-CO methods notably alter the values in the **Alpine** dataset compared to the other methods and sites. Density distribution analysis (Fig. 8b) reveals that while most methods produce similar distribution shapes, NORM results in distributions with shorter tails. In contrast, CO–CO is associated with longer tails and lower density near the mean. The IN-CO and OU-CO methods maintain density distributions closely resembling that of the RAW-D method, illustrating the nuanced effects of each correction method on the final chronology.

4. Discussion and conclusions

Different procedures to develop a chronology from raw TRSI measurements have been proposed. In our study, five correction methods have been applied to three different multi-millennial-long TRSI datasets, which resulted in different chronologies. To date, four studies have compared different methods but they used either a single dataset or short chronologies (Gagen et al., 2012; Hangartner et al., 2012; Helama et al., 2018; Labuhn et al., 2016). Our study is the first that applies, compares and evaluates five correction methods to three multi-millennial-long TRSI datasets. The three $\delta^{18}O$ datasets exhibit no evident long-term age trends, as shown in Fig. 1, consistent with previous studies (Arosio et al., 2020; Büntgen et al., 2020; Nakatsuka et al., 2020). They display distinct characteristics: the **Japanese** dataset spans the past two millennia, with fewer yet older trees; the **Central European** dataset also covers two millennia but includes trees with shorter life spans, whereas the **Alpine** dataset extends over six millennia.

The **RAW-D** method (Fig. 2a) is the most reliable for capturing low-frequency variabilities. However, the presence of outlier trees causes step changes in the composite record at beginning and end of the time series and thus affects the short-term variability. We found evident outlier trees in the **Alpine** dataset around 500 CE and in the **Japanese** dataset around 700 CE. When using this method, we recommend

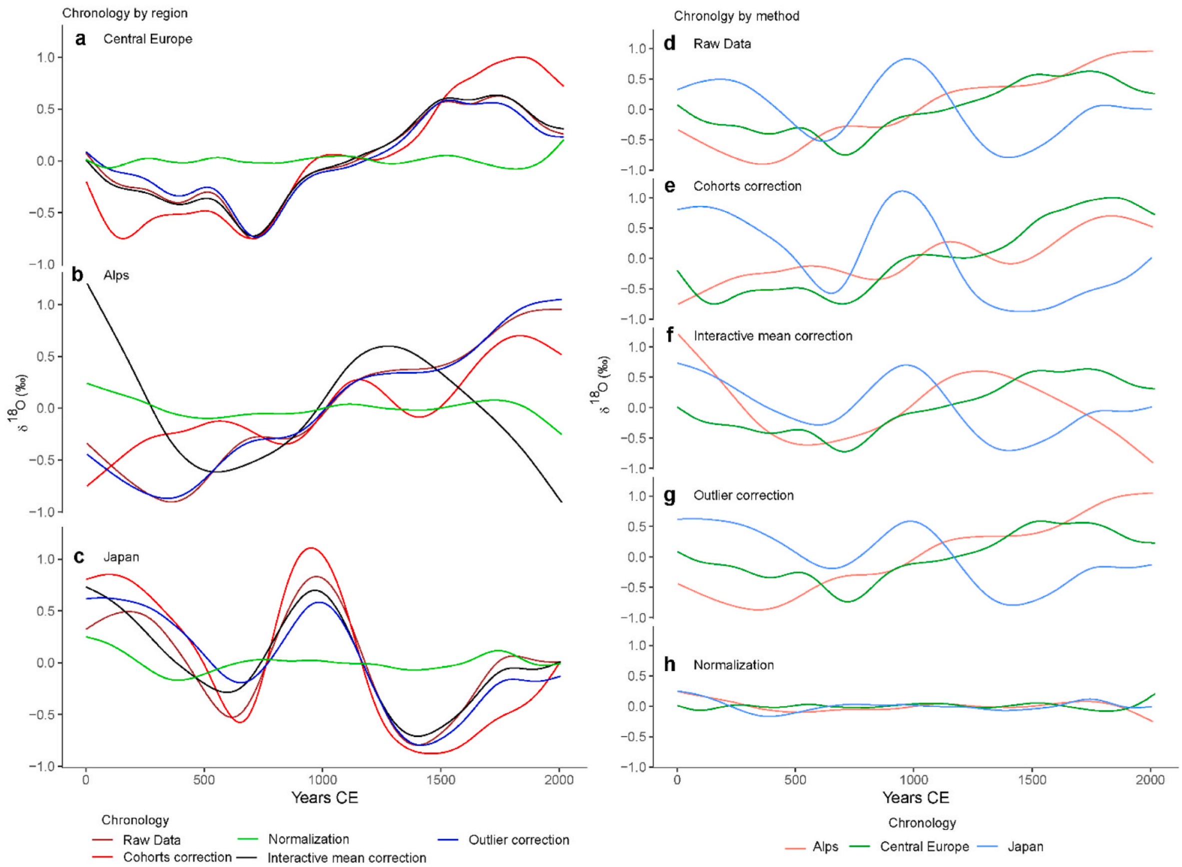

Fig. 6. Low-frequency comparison of the past 2000yrs analyzed by regions and methods. The left panel displays the 300-year spline of the various correction methods for each region from (a) Central Europe, (b) the Alps, and (c) Japan. Each line represents a different correction method: raw data (brown), cohort correction (red), interactive mean correction (black), correction of outliers (blue), and normalization (green). The right panel displays the 300-year spline of various correction methods between different regions, (d) raw data, (e) the cohort correction, (f) interactive mean correction, (g) correction of outliers, and (h) normalization. Each line represents a different correction region: Central Europe (green), the Alps (red), Japan (blue).

analysing the influence of geographical variables and outliers in the $\delta^{18}O$ mean values data to ensure that the trends are not affected by them. This method was utilized in a 6700-year precipitation reconstruction based on tree-ring $\delta^{18}O$ from the Tibetan Plateau (Yang et al., 2021) and a 2000-year hydroclimate reconstruction for Central Europe based on carbon and oxygen tree-ring isotopes (Büntgen et al., 2021), both datasets characterized by using a single tree species in a confined area.

Other methods have been developed to capture low-frequency signals and reconstruct millennial climate trends from more heterogeneous datasets without introducing steps due to averaging.

The **CO–CO** method (Fig. 2 b) assigns a high weight to the small overlap segments between series. It was suggested that frequencies that exceed the single segment should be preserved if the overlap periods are long enough to share a common variance (Hangartner et al., 2012). We found that this method produces a chronology that mostly differs from the output of all other methods (Figs. 3b, 4b and 5b, Table 2). This chronology differs from the methods RAW-D, IN-CO and OU-CO also in the low-frequency analysis (Fig. 6), and it tends to produce a different density distribution (Fig. 7c). There are two main reasons for these differences: the difficulty of prioritizing cohorts when there are several series in the same period and the high weight of short time sections. In short, a few centuries-long chronologies produced results similar to the NORM method (Labuhn et al., 2016), but this was not found in the present work. It has been successfully used for a 1000-year $\delta^{18}O$ chronology for paleoclimatic reconstruction with a careful selection of trees with a constant overlap period. However, the strategy can hardly be applied to multi-millennial tree ring records. Our results show it to be unreliable in a standard multi-millennial TRSI dataset.

The **IN-CO** method (Fig. 2c) is based on the assumption that the absolute isotope ratios of individual trees depend mainly on their location and that the temporal variations among different trees are well correlated due to a common regional climate signal. However, climate changes are expected to be reflected in low-frequency variations of tree absolute isotopic ratios (Nakatsuka et al., 2020). Our results indicate that the method works well for an annually resolved dataset, matching the information of the RAW-D and the NORM chronologies, as shown by the correlation and low-frequency analyses (Table 2, Fig. 6). However, it does not perform well with the low-time resolution datasets, such as the **Alpine** dataset, where it produces a long-term trend that is opposite to that of the chronologies produced by RAW-D and the other correction methods (Figs. 4 and 6b). The iterative repetition makes this opposite trend even stronger (Fig. S1). This method appears to affect the centennial variability in the **Alpine** dataset, in particular the period around 2600 BCE where it shows the highest values in the 6000 years, higher than those of RAW-D, OU-CO and NORM chronologies (Fig. 4). This suggests that the IN-CO method may introduce artefacts into a chronology (Fig. 4c).

The method's limitations in low-resolution datasets are attributed to the reduced number of data points in the inter-series overlaps, which results in grouping trees of the same time with similar averages and creating jumps between the overlap periods. Altogether, the method could produce reliable for building chronologies only on datasets with annual resolution.

The **IN-CO** method was developed and applied for a 2600-years hydroclimate reconstruction based on hydrogen and oxygen tree-ring isotopes from central Japan (Nakatsuka et al., 2020) and was applied

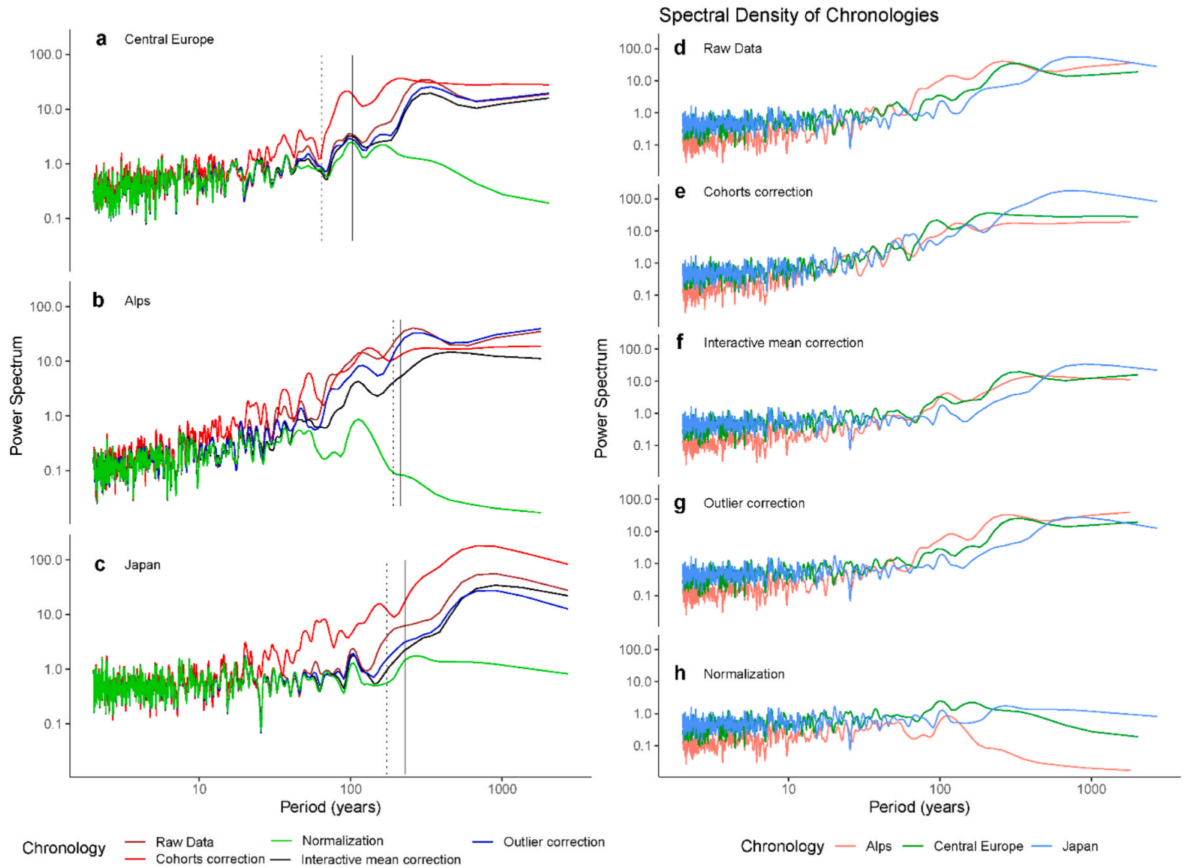

Fig. 7. Spectral analysis. Left panel shows a comparative spectral density analysis of the three different geographic regions: (a) Central Europe, (b) the Alps, and (c) Japan. Each line represents a different correction method: raw data (brown), cohort correction (red), interactive mean correction (black), correction of outliers (blue), and normalization (green). The dotted vertical line represents the median segment length, and the vertical line is the mean segment length for each dataset. Right panel displays density analysis of the various correction methods between different regions:, (d) D raw data, (e)E the cohort correction, (f)F interactive mean correction, (g) G correction of outliers and H(h) normalization. Each line represents a different correction region: Alps (red), Central Europe (green), the Alps (red), Japan (blue).

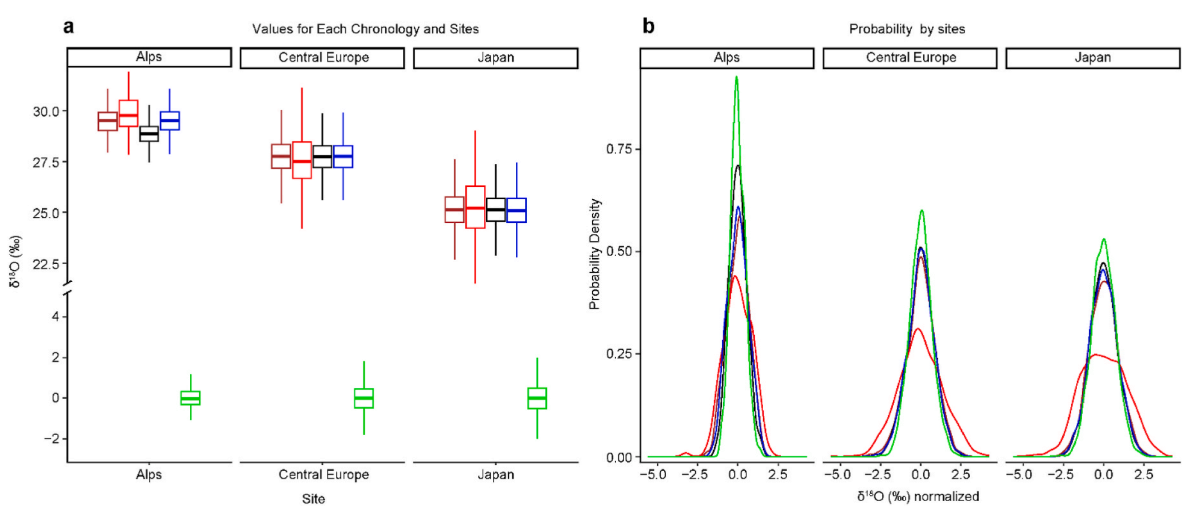

Fig. 8. Analysis of the values and density distribution of the three sites produced by the different methods. Panel a shows the boxplots of the values across the three sites of the five correction methods: method RAW-D (brown), method CO-CO (red), method IN-CO (black), method OU-CO (blue), and NORM (green). The boxplot compactly displays the distribution of variables showing the median, two hinges and two whiskers. **Panel b** presents the probability density by sites; all chronologies are corrected to have the mean value of 0. Each colour represents a different correction method, as in panel a.

to a 700-year TRSI chronology from Europe based on oxygen tree-ring isotopes (Nagavciuc et al., 2022) (Table 1).

The **OU-CO** method (Fig. 2 d) was developed to correct outlier trees that do not overlap with other series. It identifies the outlier trees based on the calibration period parameters, which, in our case, are the variance of the raw data in the climate calibration period. This method is less

Table 3
Autocorrelation analysis for each chronology (AR1). The highest (lowest) numbers for each chronology are highlighted in bold (undeline).

AR1	RAW-D	CO–CO	IN-CO	OU-CO	NORM
Center Europe	0.55	**0.75**	0.49	0.49	0.27
European Alps	0.64	**0.70**	0.47	0.60	0.21
Japan	0.44	**0.74**	0.34	0.36	0.06

corrective than the methods CO–CO, IN-CO, and NORM. In the two annually resolved datasets, it produces an outcome similar to that of the IN-CO method (Fig. 6). It captures the low-frequency signals on the lower time-resolution dataset, as the RAW-D. It was successfully applied to retain a long-term climate signal by correcting only the "outlier trees" that can affect the centenary variability of the raw data (Arosio et al., 2024).

The **NORM** method (Fig. 2e), which has the strongest correction among the methods, erases the noise provoked by the tree offsets. We confirm that it erases the low frequency from the chronologies, while the high-frequency signal is maintained only in a period shorter than the mean tree length (Fig. 7a, b, c). It is not well-suited for the present multi-millennial chronologies, in which the 200-yrs mean tree length is too short to capture the multi-millennial climate variation. It is the only method that drastically changes the mean value of the RAW-D data (Fig. 7a), which is a baseline for comparison with other sites (Saurer et al., 2002; Xu et al., 2024). The NORM method has been applied to the shorter datasets and/or for studying high-frequency climate signals where the low-frequency component was not the primary interest (Labuhn et al., 2016; Sidorova et al., 2019) (Table 1).

A hypothetical ideal dataset with evenly distributed samples across time and no major offset between samples would not require any correction methods, but the real datasets need corrections, which affect the final chronology, as shown in this study. The selection of the correction method should be based on the characteristics of the dataset. The main challenge is to preserve the low-frequency signals in TRSI datasets with trees from different areas that may have different mean isotopic values, considering that the replication of these datasets is typically of 4–6 samples. Our findings advocate for an initial utilization of raw data **(RAW-D),** complemented by geographical variable analysis and validated by the absence of outlier trees. Other methods may be appropriate under specific research questions or characteristics of the datasets. The most robust correction, i.e. the normalization **(NORM)**, removes the climate signal longer than the mean segment length. The cohort correction **(CO–CO)** is suited only for chronologies with constant inter-series overlapping; the interactive mean correction **(IN–CO)** method is suitable for annually resolved datasets, but it loses the information of the original data range that can be used to quantify the error. The outliers correction **(OU–CO)** method is preferable for situations with lower temporal resolution, but it is also reliable for annually resolved datasets.

Author contributions

T.A. and U.B. designed the study. T.A. and M.T. performed the statistical analyses. T.A. and U.B. wrote the manuscript with the help of M. T., J.E., A.K, and T.B. T.A., M.L. and K.N. processed and measured the stable isotopes on the Alpine dataset. O.U. processed and measured the stable isotopes of the Central European dataset. T.N. and M.S processed and measured the stable isotopes of the Japanese dataset. All authors provided critical discussion, helped to write and revise the manuscript and approved its submission.

Declaration of competing interest

The authors declare that they have no known competing financial interests or personal relationships that could have appeared to influence the work reported in this paper.

Data availability

The Alpine TRSI data are available on Pangaea: https://doi.org/10.1594/PANGAEA.941604. The Central European TRSI data are available on NOAA: https://www.ncdc.noaa.gov/paleo/study/32292. The Japanese TRSI data are available on NOAA: https://www.ncei.noaa.gov/access/paleo-search/study/28832.

Acknowledgements

This research has been supported by the Swiss National Science Foundation (# SNF P500PN 210716). UB received additional support from the ERC Advanced Grant (# 882727; Monostar), and the ERC Synergy Grant (# 101118880; Synergy-Plague), as well as from the Czech Science Foundation (# 23-08049S; Hydro8). TB was funded by the Hill Foundation Cambridge Trust.

Appendix A. Supplementary data

Supplementary data to this article can be found online at https://doi.org/10.1016/j.quascirev.2024.108861.

References

Arosio, T., Leuenberger, M., Nicolussi, K., Esper, J., Krusic, P., Bebchuk, T., Tegel, W., Hafner, A., Kirdyanov, A., Schluchter, C., Reinig, F., Muschitiello, F., Büntgen, U., 2024. Tree-ring stable isotopes reveal a Holocene-long drying trend for central Europe. Submitted to Science Advances.

Arosio, T., Affolter, S., Nicolussi, K., Sigl, M., Ziehmer-Wenz, M.M., Schlüchter, C., Schaad, E., Stähli, R., Leuenberger, M.C., 2022. Variable response in alpine tree-ring stable isotopes following volcanic eruptions in the tropics and Iceland. Geosciences 12, 371.

Arosio, T., Ziehmer, M.M., Nicolussi, K., Schlüchter, C., Leuenberger, M., 2020. Alpine Holocene tree-ring dataset: age-related trends in the stable isotopes of cellulose show species-specific patterns. Biogeosciences 17, 4871–4882.

Bloomfield, P., Nychka, D., 1992. Climate spectra and detecting climate change. Climatic Change 21, 275–287. https://doi.org/10.1007/BF00139727.

Briffa, K.R., Jones, P.D., Schweingruber, F.H., Karlén, W., Shiyatov, S.G., 1996. Tree-ring variables as proxy-climate indicators: problems with low-frequency signals. In: Jones, P.D., Bradley, R.S., Jouzel, J. (Eds.), Climatic Variations and Forcing Mechanisms of the Last 2000 Years. Springer Berlin Heidelberg, Berlin, Heidelberg, pp. 9–41. https://doi.org/10.1007/978-3-642-61113-1_2.

Büntgen, U., 2022. Scrutinizing tree-ring parameters for Holocene climate reconstructions. Wiley Interdisciplinary Reviews: Clim. Change e778.

Büntgen, U., Kolář, T., Rybníček, M., Koňasová, E., Trnka, M., Ač, A., Krusic, P.J., Esper, J., Treydte, K., Reinig, F., Kirdyanov, A., Herzig, F., Urban, O., 2020. No age trends in oak stable isotopes. Paleoceanogr. Paleoclimatol. 35 https://doi.org/10.1029/2019PA003831.

Büntgen, U., Urban, O., Krusic, P.J., Rybníček, M., Kolář, T., Kyncl, T., Ač, A., Koňasová, E., Čáslavskỳ, J., Esper, J., 2021. Recent European drought extremes beyond Common Era background variability. Nat. Geosci. 14, 190–196.

Cook, E.R., Briffa, K.R., Meko, D.M., Graybill, D.A., Funkhouser, G., 1995. The'segment length curse'in long tree-ring chronology development for palaeoclimatic studies. Holocene 5, 229–237.

Cook, E.R., Kairiukstis, L.A., 1990. Methods of Dendrochronology: Applications in the Environmental Sciences. Springer Science & Business Media.

Coplen, T.B., 1994. Reporting of stable hydrogen, carbon, and oxygen isotopic abundances (technical report). Pure Appl. Chem. 66, 273–276.

Duffy, J.E., McCarroll, D., Loader, N.J., Young, G.H., Davies, D., Miles, D., Bronk Ramsey, C., 2019. Absence of age-related trends in stable oxygen isotope ratios from oak tree rings. Global Biogeochem. Cycles 33, 841–848.

Esper, J., Cook, E.R., Krusic, P.J., Peters, K., Schweingruber, F.H., 2003. Tests of the RCS method for preserving low-frequency variability in long tree-ring chronologies. Tree-Ring Res. 59, 81–98.

Esper, J., Cook, E.R., Schweingruber, F.H., 2002. Low-frequency signals in long tree-ring chronologies for reconstructing past temperature variability. Science 295, 2250–2253. https://doi.org/10.1126/science.1066208.

Esper, J., Frank, D.C., Battipaglia, G., Büntgen, U., Holert, C., Treydte, K., Siegwolf, R., Saurer, M., 2010. Low-frequency noise in δ^{13} C and δ^{18} O tree ring data: a case study of *Pinus uncinata* in the Spanish Pyrenees: noise in δ^{13}C and δ^{18}O data. Global Biogeochem. Cycles 24. https://doi.org/10.1029/2010GB003772 n/a-n/a.

Esper, J., Frank, D.C., Timonen, M., Zorita, E., Wilson, R.J., Luterbacher, J., Holzkämper, S., Fischer, N., Wagner, S., Nievergelt, D., 2012. Orbital forcing of tree-ring data. Nat. Clim. Change 2, 862–866.

Esper, J., Holzkämper, S., Büntgen, U., Schöne, B., Keppler, F., Hartl, C., George, S.S., Riechelmann, D.F., Treydte, K., 2018. Site-specific climatic signals in stable isotope records from Swedish pine forests. Trees (Berl.) 32, 855–869.

Esper, J., Schneider, L., Smerdon, J.E., Schöne, B.R., Büntgen, U., 2015. Signals and memory in tree-ring width and density data. Dendrochronologia 35, 62–70.

Fritts, H., 1976. Tree Rings: Basics and Applications of Dendrochronology. Springer Science & Business Media.

Gagen, M., McCarroll, D., Jalkanen, R., Loader, N.J., Robertson, I., Young, G.H.F., 2012. A rapid method for the production of robust millennial length stable isotope tree ring series for climate reconstruction. Global Planet. Change 82, 96–103.

Hangartner, S., Kress, A., Saurer, M., Frank, D., Leuenberger, M., 2012. Methods to merge overlapping tree-ring isotope series to generate multi-centennial chronologies. Chem. Geol. 294, 127–134.

Helama, S., Arppe, L., Timonen, M., Mielikäinen, K., Oinonen, M., 2018. A 7.5 ka chronology of stable carbon isotopes from tree rings with implications for their use in palaeo-cloud reconstruction. Global Planet. Change 170, 20–33.

Kagawa, A., Sano, M., Nakatsuka, T., Ikeda, T., Kubo, S., 2015. An optimized method for stable isotope analysis of tree rings by extracting cellulose directly from cross-sectional laths. Chem. Geol. 393, 16–25.

Kirdyanov, A.V., Treydte, K.S., Nikolaev, A., Helle, G., Schleser, G.H., 2008. Climate signals in tree-ring width, density and $\delta^{13}C$ from larches in Eastern Siberia (Russia). Chem. Geol. 252, 31–41.

Labuhn, I., Daux, V., Girardclos, O., Stievenard, M., Pierre, M., Masson-Delmotte, V., 2016. French summer droughts since 1326 CE: a reconstruction based on tree ring cellulose $\delta^{18}O$ O. Clim. Past 12, 1101–1117. https://doi.org/10.5194/cp-12-1101-2016.

Leavitt, S.W., 2010. Tree-ring C–H–O isotope variability and sampling. Sci. Total Environ. 408, 5244–5253.

McCarroll, D., Loader, N.J., 2004. Stable isotopes in tree rings. Quat. Sci. Rev. 23, 771–801.

McGill, R., Tukey, J.W., Larsen, W.A., 1978. Variations of box plots. Am. Statistician 32, 12–16. https://doi.org/10.1080/00031305.1978.10479236.

Nagavciuc, V., Ionita, M., Kern, Z., McCarroll, D., Popa, I., 2022. Ã 700 years perspective on the 21st century drying in the eastern part of Europe based on $\delta^{18}O$ in tree ring cellulose. Communications Earth & Environment 3, 277.

Nakatsuka, T., Sano, M., Li, Z., Xu, C., Tsushima, A., Shigeoka, Y., Sho, K., Ohnishi, K., Sakamoto, M., Ozaki, H., 2020. A 2600-year summer climate reconstruction in central Japan by integrating tree-ring stable oxygen and hydrogen isotopes. Clim. Past 16, 2153–2172.

Naulier, M., Savard, M.M., Bégin, C., Gennaretti, F., Arseneault, D., Marion, J., Nicault, A., Bégin, Y., 2015. A millennial summer temperature reconstruction for northeastern Canada using oxygen isotopes in subfossil trees. Clim. Past 11, 1153–1164.

Pumijumnong, N., Bräuning, A., Sano, M., Nakatsuka, T., Muangsong, C., Buajan, S., 2020. A 338-year tree-ring oxygen isotope record from Thai teak captures the variations in the Asian summer monsoon system. Sci. Rep. 10, 8966.

Sano, M., Kimura, K., Miyake, F., Tokanai, F., Nakatsuka, T., 2023. Two new millennium-long tree-ring oxygen isotope chronologies (2349–1009 BCE and 1412–466 BCE) from Japan. Radiocarbon 65, 721–732.

Saurer, M., Schweingruber, F., Vaganov, E.A., Shiyatov, S.G., Siegwolf, R., 2002. Spatial and temporal oxygen isotope trends at the northern tree-line in Eurasia. Geophys. Res. Lett. 29 https://doi.org/10.1029/2001GL013739.

Sidorova, O.V., Saurer, M., Guillet, S., Corona, C., Fonti, P., Myglan, V.S., Kirdyanov, A. V., Naumova, O.V., Ovchinnikov, D.V., Shashkin, A.V., 2019. Siberian tree-ring and stable isotope proxies as indicators of temperature and moisture changes after major stratospheric volcanic eruptions. Clim. Past 15, 685–700.

Torbenson, M., Klippel, L., Hartl, C., Reinig, F., Treydte, K., Büntgen, U., Trnka, M., Schöne, B., Schneider, L., Esper, J., 2022. Investigation of age trends in tree-ring stable carbon and oxygen isotopes from northern Fennoscandia over the past millennium. Quat. Int. 631, 105–114.

Treydte, K., Boda, S., Graf Pannatier, E., Fonti, P., Frank, D., Ullrich, B., Saurer, M., Siegwolf, R., Battipaglia, G., Werner, W., 2014. Seasonal transfer of oxygen isotopes from precipitation and soil to the tree ring: source water versus needle water enrichment. New Phytol. 202, 772–783.

Treydte, K.S., Schleser, G.H., Helle, G., Frank, D.C., Winiger, M., Haug, G.H., Esper, J., 2006. The twentieth century was the wettest period in northern Pakistan over the past millennium. Nature 440, 1179–1182. https://doi.org/10.1038/nature04743.

Urban, O., Ač, A., Kolář, T., Rybníček, M., Pernicová, N., Koňasová, E., Trnka, M., Büntgen, U., 2021. The dendroclimatic value of oak stable isotopes. Dendrochronologia 65, 125804.

Wang, L., Liu, Y., Li, Q., Song, H., Cai, Q., Sun, C., Fang, C., Liu, R., 2020. A 210-year tree-ring $\delta^{18}O$ record in North China and its relationship with large-scale circulations. Tellus B 72, 1770509. https://doi.org/10.1080/16000889.2020.1770509.

Warren, C.R., McGrath, J.F., Adams, M.A., 2001. Water availability and carbon isotope discrimination in conifers. Oecologia 127, 476–486. https://doi.org/10.1007/s004420000609.

Wieland, A., Römer, P., Torbenson, M., Greule, M., Urban, O., Čáslavskỳ, J., Pernicová, N., Trnka, M., Büntgen, U., Esper, J., 2024. Tree-ring stable isotopes in cellulose and lignin methoxy groups reveal different age-related behaviour. Quat. Int. 693, 38–48.

Xu, C., Huang, R., An, W., Zhao, Q., Zhao, Y., Ren, J., Liu, Y., Guo, Z., 2024. Tree ring oxygen isotope in Asia. Global Planet. Change 232, 104348.

Xu, G., Liu, X., Trouet, V., Treydte, K., Wu, G., Chen, T., Sun, W., An, W., Wang, W., Zeng, X., Qin, D., 2019. Regional drought shifts (1710–2010) in East Central Asia and linkages with atmospheric circulation recorded in tree-ring $\delta^{18}O$. Clim. Dynam. 52, 713–727. https://doi.org/10.1007/s00382-018-4215-2.

Yang, B., Qin, C., Bräuning, A., Osborn, T.J., Trouet, V., Ljungqvist, F.C., Esper, J., Schneider, L., Grießinger, J., Büntgen, U., 2021. Long-term Decrease in Asian Monsoon Rainfall and Abrupt Climate Change Events over the Past 6,700 Years, vol. 118. Proceedings of the National Academy of Sciences, e2102007118.

Zhao, Y., Xu, C., Liu, Y., An, W., Guo, Z., 2023. Irrawaddy River experienced more frequent hydrological drought events with global warming: evidence from a 400-year tree ring oxygen isotope record. Catena 232, 107455.

Ziehmer, M.M., Nicolussi, K., Schlüchter, C., Leuenberger, M., 2018. Preliminary evaluation of the potential of tree-ring cellulose content as a novel supplementary proxy in dendroclimatology. Biogeosciences 15, 1047–1064.